Anal. Bioanal. Electrochem., Vol. 8, No. 7, 2016, 848-861

Analytical & Bioanalytical Electrochemistry

2016 by CEE
www.abechem.com

Full Paper

Voltammetric Determination of Molecular Modeling Parameters for Pentaazamacrocyclic Complexes of Mn(II) and Co(II)

Anuj Kumar,[1,*] Vinod Kumar Vashistha,[2] Prashant Tevatia[1] and Randhir Singh[1]

[1]*Department of Chemistry Gurukula Kangri University Haridwar-249404, India*
[2]*Department of Chemistry, Institute of Applied Sciences and Humanities, GLA University, Mathura, India-281406*

*Corresponding Author, Tel.: +91-9761565732
E-Mail: anujkumar9791@gmail.com

Received: 26 May 2016 / Received in revised form: 18 September 2016 / Accepted: 1 October 2016 / Published online: 15 November 2016

Abstract- In present studies, [$Mn^{II}LCl_2$] and [$Co^{II}LCl_2$] pentaazamacrocyclic complexes (where L=Dichloro-2,3-dimethyl[b]-pyridyl-3,6,9,12,15-pentaazacyclopentadeca-2,12-diene) have been synthesized by template method and characterized by microanalysis, UV-Vis, IR and mass spectral studies. On the basis of electronic spectral studies, the saddle-shape octahedral geometry has been assigned to these pentaazamacrocyclic complexes. Electrochemical studies of HOMO-LUMO energy levels of these pentaazamacrocyclic complexes have been carried out by using cyclic voltammetry. The onset oxidation and reduction potentials of [$Mn^{II}LCl_2$] and [$Co^{II}LCl_2$] macrocyclic complexes were determined under the similar experimental conditions to calculate the ionization potential (Ip) and electron affinity (Ea) for these macrocyclic complexes. The molecular modeling parameters were also calculated from the calculation of HOMO-LUMO energy levels. The obtained values of these parameters are indicating that [$Mn^{II}LCl_2$] macrocyclic complex is more stable than [$Co^{II}LCl_2$] complex. The biological activity of these macrocyclic complexes were also taken into account against *E. coli*, *B. cereus*, *P. aeruginosa*, *S. aureus* and *C. albicans* microbial pathogen and compared with the standard drug Gentamycin.

Keywords- Spectroscopy, Cyclic voltammetry, Redox modeling, Antimicrobial

1. INTRODUCTION

The field of designing and synthesis of macrocyclic complexes of metal ions is growing day by day with desire to find out the highly polar and stable redox couple based materials for use as components in redox sensors, photo electrochemical cells, redox storage batteries and also to develop the mimic aspects of the spectral [1-4], chemical and biological properties of metal sites proteins [5]. One of the most interesting aspects of macrocyclic complexes is that the ligand can be modified by the substitution to enjoy extensive interest owing to their structural diversity and potential applications such as anticancer [6], anticonvulsant [7], anti-inflammatory [8], antitumor [9], antimicrobial [10], anti-tubercular [11-12], antioxidant, antimalarial [13-15]. These potential applications can be correlated to the position of the HOMO and LUMO energy levels, reversibility of electrochemical process and stability of the macrocyclic complexes [16-21]. The knowledge of charge carrier energy levels in macrocyclic complexes is very essential to understand the way of interaction between the ligand and metal ion and also to calculate the chemical quantum parameters which are useful to determine the nature of ligand, stability and reactivity of macrocyclic complexes. Electroluminescent conjugated macrocyclic complexes are often have a great deal of interest due to their promising commercial applications in organic light emitting diodes (OLEDs), field effect transistors, photovoltaic diodes, solar cells and electrochemical cells [22-25]. OLED usually consists of several layers of various stacked organic thin films and high energy gap between energies of separate layers which act as potential energy barriers to the flow of charge in the molecular excited states. The fine adjusting of HOMO and LUMO energy levels of different OLED's layers is very important. Electrochemical studies are suitable for multifarious applications. Moreover, in macrocyclic chemistry, cyclic voltammetry and ultraviolet photoemission spectroscopy (UPS) have been recognized as an easy and effective approach to evaluate the HOMO-LUMO energies ($E_{HOMO/LUMO}$). Solution-based cyclic voltammetry (CV) experiment is employed for determination of ionization potential (I_p) and electron affinity (E_a) of macrocyclic complex. Ionization potential (I_p) and electron affinity (E_a) may be regarded as HOMO and LUMO energy levels of molecule and can be estimated by electrochemical oxidation or reduction [26-35].

The present study describes the synthesis, characterization, calculation of electrochemical HOMO-LUMO energy levels and chemical quantum parameters; *viz* electronegativity, chemical potential, global softness/hardness and electrophilicity index for the synthetic macrocyclic complexes of Mn (II) and Co(II). The stabilization of unusual oxidation state of metal ions, heterogeneous electron transfer rate constant and diffusion have also been taken into account.

2. EXPERIMENTAL

2.1. Methods and materials

All the chemicals were of analytical reagent (AR) grade purchased from TCI India and used without further purification. The electrochemical studies were performed using a standard one-compartment three electrode electrochemical cell connected to an electrochemical analyser Auto Lab Metrohm 663 VA Stand Instrument. The working electrode was a Pt electrode (tip-6.1204.120, 0.031 cm^2) and pre-treatment of electrode was done before every experiment. Silver (Ag/0.1 M AgCl) and platinum wire electrode were used as reference and counter electrode respectively. Tetraethylammonium perchlorate (TEAP) was used as supporting electrolyte. The energies of the HOMO-LUMO levels were determined from the first oxidation and reduction potentials, respectively, by taking the known E_{HOMO} of Ferrocene (4.8 eV below the vacuum level) as reference value. The E_{ox} of ferrocene *vs* Ag/AgCl internal standard was measured to be -0.48 V and $E_{HOMO/LUMO}$ values for these macrocycles were calculated according to the following equation (1).

$$E_{HOMO/LUMO}\ (eV) = -\{E_{redox} - (0.48\ eV)\} - 4.8\ eV \quad \text{(Eq. 1)}$$

Optical HOMO-LUMO gap for both the macrocycles were also measured by UV-Vis spectroscopy in dimethylsulphoxide (DMSO). The onset of the longest wavelength absorption was used to determine the optical band gap (E_g) according to the following equation (2).

$$E_g = 1240/\lambda_{onset} \quad \text{(Eq. 2)}$$

2.2. Preparation of the macrocycles

Pentaazamacrocyclic complexes have been synthesized according to the literature method [36-37].

2.2.1. Synthesis of $[Mn^{II}LCl_2]$ and $[Co^{II}LCl_2]$ tetraazamacrocyclic complexes

To a methanolic solution (25 ml) of triethyltetraamine (TETA) (0.292 g/0.31 ml) in a round bottom flask and added to a methanolic solution (25 ml) of 2,6-diacetylpyridine (0.326 gm) was stirring followed by addition of methanolic solution of metal salts [$MnCl_2.4H_2O$ (0.198 g)/ $CoCl_2.6H_2O$ (0.476 gm)] in 2:2:2 molar ratio. The obtained mixtures were refluxed for 6 hours, a change in color was observed, the solution was concerted on rotary evaporator upto dryness with methanol. The scheme for synthesis is given in Fig.1 and the analytical data given below.

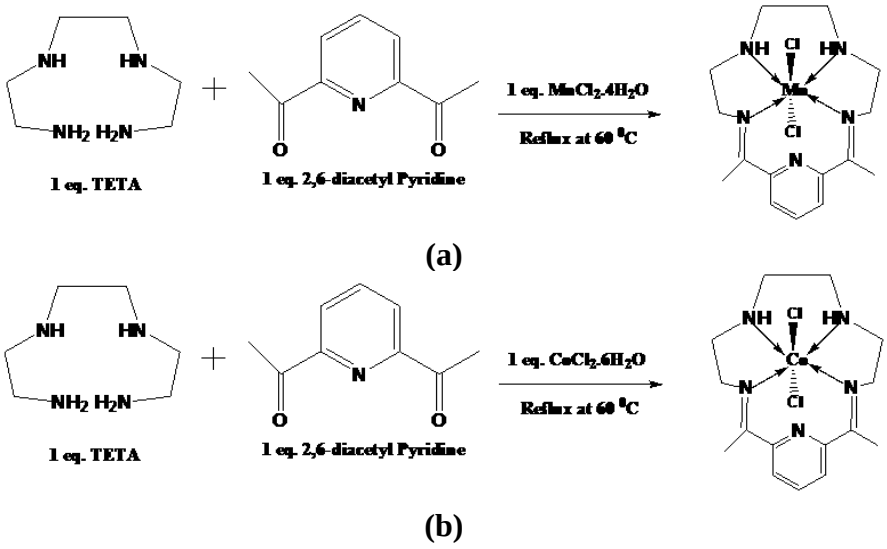

Fig. 1. Synthesis scheme of Dichloro-2,3-dimethyl[b]pyridyl-3,6,9,12,15-Pentaaza-cycloPentadeca-2,12-dienemacrocycles of (a) Mn(II) [$Mn^{II}LCl_2$] and (b) Co(II) [$Co^{II}LCl_2$]

2.3. Analytical data of [$Mn^{II}LCl_2$] and [$Co^{II}LCl_2$] macrocyclic complexes

[$Mn^{II}LCl_2$]: Yield: 0.18 g (74%); M.pt: 215 °C; LC-MS spectra of this complex showed molecular ion peak at m/z 399, base peak at m/z 328 and other peaks are observed at m/z 71, 78,132.

[$Co^{II}LCl_2$]: Yield: 0.19 g (75%); M.pt: 235 °C; LC-MS spectra of this macrocyclic complex showed molecular ion peak at m/z 403, base peak at m/z 332 and some other peaks are also observed.

2.4. Preparation of microbial cultures for biological activities

The microbial cultures for these pentaazamacrocyclic complexes were adjusted to 0.5 McFarland standards; microbial pathogen suspension of approximately 1.5×10^8 cfu/ml, 30 of agar media were poured into four petri plates and was swabbed with 100 µl microbial inoculums for the test microorganisms and kept for one hour. A 6 mm well was cut at the centre of each agar plates and were filled with the 10^{-3} M solution of macrocyclic complexes. The solvent medium (DMSO) was used as a negative control whereas media with the standard drug (Gentamycin) used as positive control, all prepared culture's petri plates were placed in incubation at 37 °C for 24 hours and in case for fungus, it was kept for 48 hours at 28 °C.

3. RESULT AND DISCUSSION

The observed data of microanalysis are in the agreement with the composition. The macrocyclic complexes are highly soluble in methanol, dimethylformamide (DMF) and

dimethylsulphoxide (DMSO). The physical properties of both macrocyclic complexes are given in table 1.

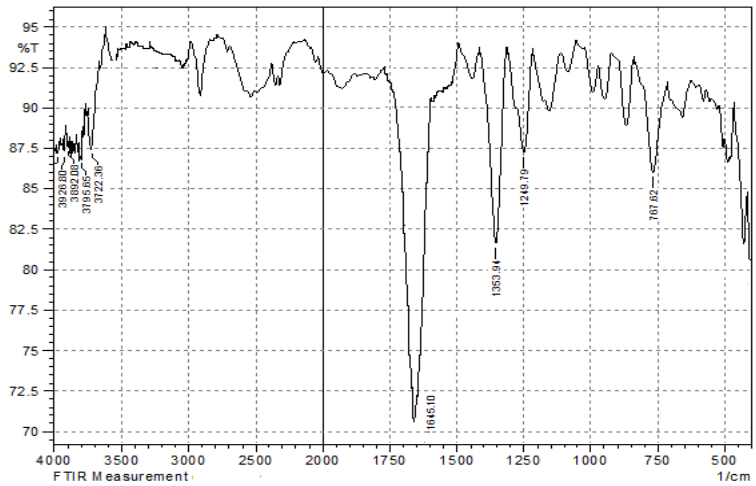

(a)

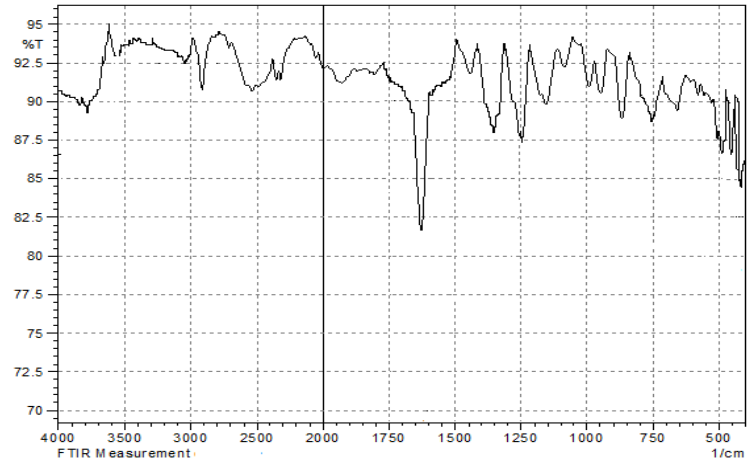

(b)

Fig. 2. IR spectra of (a) $[Mn^{II}LCl_2]$ macrocyclic complex and (b) $[Co^{II}LCl_2]$ macrocyclic complex

Table 1. Physical properties of $[Mn^{II}LCl_2]$ and $[Co^{II}LCl_2]$ macrocyclic complexes

Complexes	**Color**	**Mol. Cond. ($Ohm^{-1}cm^2$ mol^{-1})**	**Shape**	**C (found) (%)**	**H (found) (%)**	**N (found) (%)**
$[Mn^{II}LCl_2]$	Light yellow	47	Octahedral	44.66 (43.34)	05.70 (04.57)	17.36 (17.16)
$[Co^{II}LCl_2]$	Brown	36	Octahedral	44.66 (43.25)	05.70 (4.73)	17.36 (17.13)

3.1. Spectral studies

IR spectra for both the macrocyclic complexes were recorded in the range of 400-4000 cm^{-1}. The IR spectra of both macrocyclic complexes showed an intense band near 1625-1650 cm^{-1} due to *ν*(C=N) group. The characteristic bands (Fig. 2a and 2b) observed in the region 1575-1590 cm^{-1}, 700-900 cm^{-1} and 2930-3000 cm^{-1} may be assigned for the stretching vibrations of *ν*(C=C), *ν*(-CH_2-) units and *ν*(C-H) stretching of methyl groups respectively. The other absorption characteristics also appeared in the region 520-570 cm^{-1} which may be assigned for *ν*(M-N) vibrations. The IR data for these macrocyclic complexes is given in table 2.

Table 2. IR data of both [$Mn^{II}LCl_2$] and [$Co^{II}LCl_2$] macrocyclic complexes

Macrocyclic complexes	**>C=N str.**	**C=C str. (Aromatic)**	**C—H str. (Methyl)**	**M—N str.**
[$Mn^{II}LCl_2$]	1645	1353,1249	2935	560
[$Co^{II}LCl_2$]	1630	1375, 1255	2985	495

3.2. Optical absorption band gap studies

UV-Vis absorption spectroscopy is very useful to obtain the band gap energy potential (E_g). This energy gap showed the energy difference between HOMO-LUMO in the molecule. The band gaps (E_g) for these macrocyclic complexes were determined by extrapolating in the UV-Vis spectra.

Electronic spectra of these macrocyclic complexes were recorded in DMSO. Both the spectra are quite different. The spectrum of [$Mn^{II}LCl_2$] complex showed a longer absorption band at 15,873 cm^{-1} (ε=24 L mol^{-1} cm^{-1}) which can be assigned to $^6A_{1g} \rightarrow {}^4A_{1g}$ (4G) while other weak intense bands were observed at 21,256 cm^{-1} (ε=33 mol^{-1} cm^{-1}), 23,985 cm^{-1} (ε=61 L $mol^{-1}cm^{-1}$). These bands may be assigned to $^6A_{1g} \rightarrow {}^4E_g$, $^6A_{1g}$ (4G) transition (10B+5C), $^6A_{1g} \rightarrow {}^4E_g$ (4D) (17B+5C) and $^6A_{1g} \rightarrow {}^4T_{1g}$ (4P) transitions respectively. The electronic spectrum of [$Co^{II}LCl_2$] macrocyclic complex also showed a longer absorption band at 14598 cm^{-1} which can be assignable to $^4T_{1g}(F) \rightarrow {}^4T_{1g}$ (P) transition and other observed two bands are in region 31769 cm^{-1} and 29818 cm^{-1}. These bands can be assigned to $^4T_{1g}$ (F)$\rightarrow {}^4A_{2g}$(F), $^4T_{1g}(F) \rightarrow {}^4T_{2g}$ (F) transitions respectively. The electronic spectral data and molar conductance data of these macrocyclic complexes suggest the octahedral geometry for both the macrocyclic complexes, the chloride ions being at the axial positions. The onset wavelengths for these transitions of [$Mn^{II}LCl_2$] and [$Co^{II}LCl_2$] were determined at 740 nm and 755 nm respectively by drawing the intersection of the two tangents drawn at the rising current of the

UV-Vis traces. The band gap energies of these transitions and the position of LMCT transition in eV can be calculate by using the equation 3 and 4.

$$E\ (J) = hc/(m) \qquad E\ (eV) = 1239.84\ eV\ (nm)/(nm)$$

$$E\ (eV) = 1240\ eV/\ \lambda_{onset} \qquad \text{(Eq. 3)}$$

$$\Delta E\ (LMCT) \approx E\ (L/L^{+}) - E\ (Mn^{+1/n+}) \qquad \text{(Eq. 4)}$$

Where, E (L/L^{+}): ligand redox potential and E ($Mn^{+1/n+}$): metal redox potential

3.3. Electrochemical studies

The redox behaviour of these macrocyclic complexes were studied by employing cyclic voltammetry. All the voltammograms (CVs) of these complexes were recorded under the nitrogen atmosphere in DMSO (10^{-3}) containing 0.1 M TEAP as a supporting electrolyte and the scan rate was maintained 50-250 mVs^{-1}. The diffusion coefficient (D_0) and heterogeneous electron transfer rate constant (K^0) for both macrocyclic complexes have been calculated with the help of Nicholson and Kochi methods.

The typical cyclic voltammogram of $[Mn^{II}LCl_2]$ macrocyclic complex was recorded at a scan rate of 200 mVs^{-1} and shown in Fig. 3a. The voltammogram show an intense anodic peak (Ia) at -0.52 V and one cathodic peak at -0.44 V. On the basis of peak separation (ΔE=0.08 V) and peak current ratio ($i_{pa}/i_{pc} \approx 1$), the corresponding redox couple (Ia/Ic) can be assigned to one electron transfer quasirreversible redox process Mn^{+}/Mn^{+2} with the formal potential at -0.50 V. A distinct anodic peak is also observed at +0.18 V which may be assigned to the oxidation process of $Mn^{+2} \rightarrow Mn^{+3}$. Another observed corresponding redox couple (IIIa/IIc) at +1.07 V formal potential is assignable to the ligand oxidation redox process (L/L^{+}).

Similarly, the cyclic voltammogram of $[Co^{II}LCl_2]$ macrocyclic complex was also recorded in similar conditions at a scan rate of 200 mVs^{-1} and shown in Fig. 3b. The voltammogram shows two anodic peaks (Ia and IIa) at -0.57 V and -0.25 V while on reverse scanning two cathodic peaks (Ic and IIc) were observed at -0.48 V and +0.23 V respectively. On the basis of peak separation (ΔE=0.09 V) and peak current ratio ($i_{pa}/i_{pc} \approx 1$), the corresponding redox couple (Ia/Ic) has been assigned to one electron reversible redox process of Co/Co^{+} with the -0.45 V formal potential. The observed another corresponding redox couple (IIa/IIc) assigned to a totally irreversible redox couple Co^{+}/Co^{2+}.

The dependence of peak current and potential at scan rate (v) between 50-250 mVs^{-1} also has been taken into account. For both macrocyclic complexes, the plots of I_p *vs* $v^{1/2}$ are found as linear for one electron transfer redox processes of these macrocyclic complexes which are indicating that the diffusion phenomenon follows by Randles-Sevcik equation (Eq. 5) while the shifting in the peak position with increasing scan rate (v) indicates the kinetic effects. The

current response for rest of the peaks was not observed clearly proportional to scan rate (v) and also $v^{1/2}$.

$$i = 2.69 \times 10^5 \, n^{3/2} A \, D^{1/2} c v^{1/2} \qquad \text{(Eq. 5)}$$

Where n is the number of electrons transferred, A is the area of electrode, D is the diffusion coefficient, c is the concentration of electroactive species and v is the scan rate.

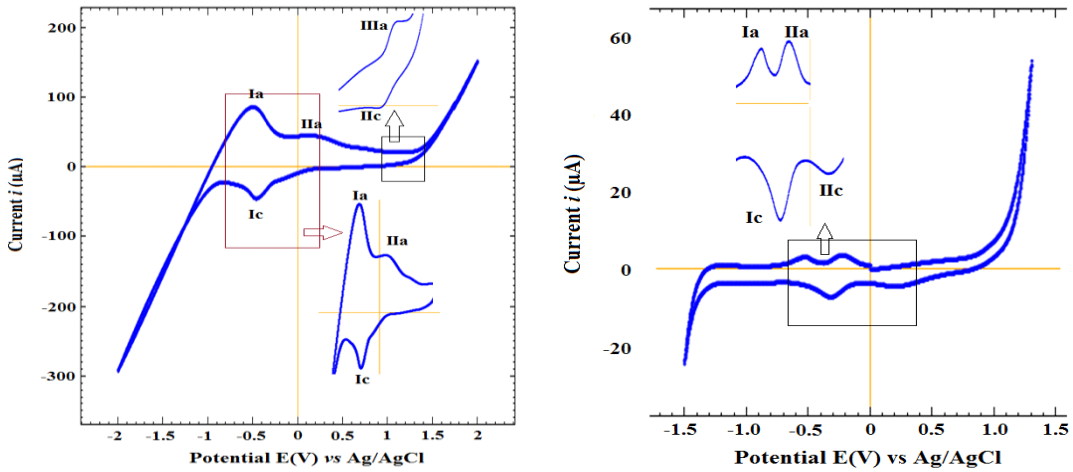

Fig. 3. Cyclic voltammograms of (a) [$Mn^{II}LCl_2$] and (b) [$Co^{II}LCl_2$] macrocyclic complexes in DMSO containing 10^{-3} M of complex and 0.1 M TEAP as supporting electrolyte at a scan rate of 200 mV

The theoretical values of diffusion coefficient (D_0) and heterogeneous electron transfer rate constant (K^0) were calculated at 200 mVs^{-1} scan rate using Nicholson and Kochi methods which were found in the decreasing order $D_0^{Co(II)}$ (1.51×10^{-5} cm^2/s) > $D_0^{Mn(II)}$ (1.03×10^{-5} cm^2/s) and $K^0_{Mn(II)}$ (3.17×10^{-3} cm/s) > $K^0_{Co(II)}$ (2.49×10^{-3} cm/s) respectively.

3.4. Study of E_{HOMO} and E_{LUMO} energy levels

Cyclic voltammetry is very useful technique to determine HOMO-LUMO or band gaps energy for an electroactive species. When an electroactive molecule is oxidised, one electron out of the HOMO energy level transferred into the LUMO energy level during the redox process (a strongly bound electron-hole pair is created), as a result the energy of an unoccupied site changes upon occupation but it depends on the kind of process/ device.

Thus the gap energy between both peak potential (eV) multiply by electronic charge suggest the HOMO-LUMO energy gap. For these macrocyclic complexes, the HOMO and LUMO energy levels were calculated by using the equation 6 and 7. [14]

$$\text{HOMO (or LUMO) (eV)} = -4.8 - [(E_{peak\ potential} - E_{1/2}\ (\text{Ferrocene})] \qquad \text{(Eq.6)}$$

$$E_{HOMO} = - (1.4 \pm 0.1)\ q\ V_{CV} - (4.6 \pm 0.08)\ eV \qquad \text{(Eq.7)}$$

Where, $E_{peak\ Potential}$ are the maximum and minimum peak potential and $E_{1/2}$ is the half-wave potential of Ferrocene (0.42 V); V_{CV} is the molecular oxidation potential from CV and q is the charge of an electron.

In this investigation, the observed values of onset potentials for oxidation and reduction peaks from the cyclic voltammograms of these macrocyclic complexes were used to determine the ionization potential (IP), electron affinity (Ea) and energy gap (E_g) by using following equations (8, 9 and 10)

$$I_p = - (E_{ox} + 4.4)\ eV \qquad \text{(Eq. 8)}$$

$$E_a = - (E_{red} + 4.4)\ eV \qquad \text{(Eq. 9)}$$

$$E_g = I_p - Ea \qquad \text{(Eq. 10)}$$

Where E_{ox} and E_{red} are the onset potentials oxidation and reduction peaks respectively while E_g is the band gap. Onset potentials are determined by the polating in cyclic voltammograms. Fig. 4 was used only for the representation of onset potentials (the intersection point potential of the two tangents drawn at the rising current and the base line charging current of the CV traces) by using the cyclic voltammogram of standard.

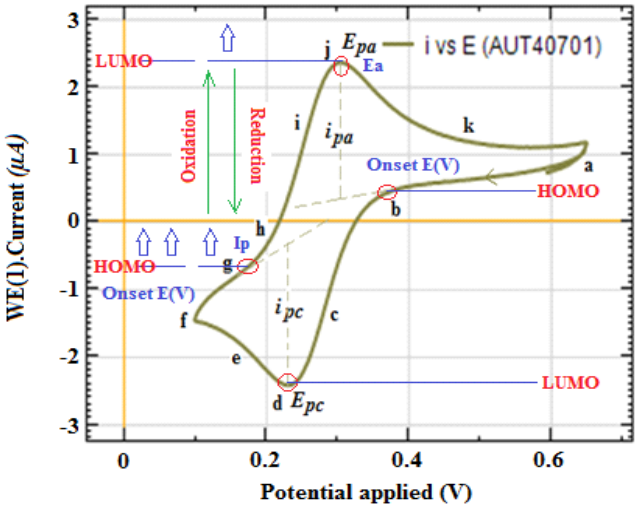

Fig. 4. Cyclic voltammogram of standard $[Fe(CN)_6]^{3+}$: Graphical representation for the determination of onset potentials and HOMO-LUMO energy levels

The cyclic voltammograms of $[Mn^{II}LCl_2]$ and $[Co^{II}LCl_2]$ macrocyclic complexes were recorded in DMSO and shown in Fig. 5a and 5b. The peak potentials and onset potentials were obtained from the voltammograms and given in table 3 which was considered for the calculation of HOMO-LUMO energy levels. On the basis of observed data, the oxidation and reduction peaks can be correlated directly to electron transfer at HOMO to LUMO

respectively. The observed data was used for the calculation of molecular redox modelling parameters of these macrocyclic complexes.

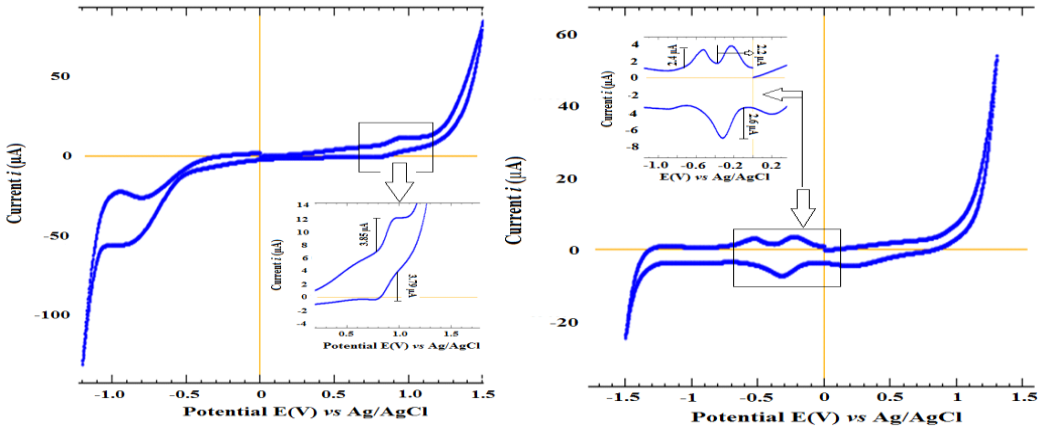

(a) **(b)**

Fig. 5. Cyclic voltammograms of (a) $[Mn^{II}LCl_2]$ and (b) $[Co^{II}LCl_2]$ macrocyclic complexes in DMSO containing 10^{-3} M of complex and 0.1 M TEAP as supporting electrolyte at a scan rate of 200 mVs^{-1}. The inserted voltammograms showed the onset potentials and enlarge of major redox couple

3.5. Study of molecular modelling parameters

The molecular modelling parameters; electronegativity (χ), global hardness (η), global softness (σ), chemical potential (μ) and global electrophilicity index (ω) for these macrocyclic complexes were obtained from the calculation of highest occupied molecular level (E_{HOMO}) and energy of lowest unoccupied molecular level (E_{LUMO}). The data is given in table 3. The electrophilicity index parameter play an important role to quantify the biological activity of drug receptor interaction and the observed values of biological activities against pathogens are in the agreement with their electrophilicity index.

Table 3. Molecular modelling parameters of the macrocyclic complexes

Macrocycles	**E_{HOMO}**	**E_{LUMO}**	**ΔE**	**X**	**η**	**σ**	**Ω**	**μ**	**ΔN_{Max}**
$[Mn^{II}LCl_2]$	-3.9	-4.5	0.6	4.2	0.3	3.3	28.9	-4.2	14
$[Co^{II}LCl_2]$	-4.1	-3.1	1.0	3.6	0.5	1.9	12.7	-3.6	7.0

Where $\chi = -1/2 [E_{HOMO} + E_{LUMO}]$, $\mu = -\chi = 1/2 [E_{HOMO} + E_{LUMO}]$, $\eta = 1/2 [E_{HOMO}-E_{LUMO}]$, $\omega = \mu^2/2\eta$ and $\Delta N_{Max} = -\chi/\eta$

The global hardness and its inverse parameters are very important to measure the stability and reactivity of the complexes. These parameters also give an idea about the unsaturation in the macrocyclic frame work. The unsaturation in the macrocyclic frame can also be

determined with the help of $\Delta E_{1/2}$ value. The observed high value of E_{HOMO} and E_{LUMO} energy gap for $[Mn^{II}LCl_2]$ macrocyclic complex is indicating that $[Mn^{II}LCl_2]$ macrocyclic complex is globally hard than $[Co^{II}LCl_2]$ macrocyclic complex. Thus $[Mn^{II}LCl_2]$ macrocyclic complex is more stable or less reactive than $[Co^{II}LCl_2]$ macrocyclic complex. Due to high energy gap for $[Mn^{II}LCl_2]$ macrocyclic complex, it could not easily offer the electron to an acceptor which is also supported by the observed high value of chemical potential parameter (μ).

3.6. Biological activities

The antimicrobial activities of the $[Mn^{II}LCl_2]$ and $[Co^{II}LCl_2]$ macrocyclic complexes were studied by agar well diffusion method against *E. coli, P. aeruginosa, B. cereus, S. aureus and C. albicans* pathogens.

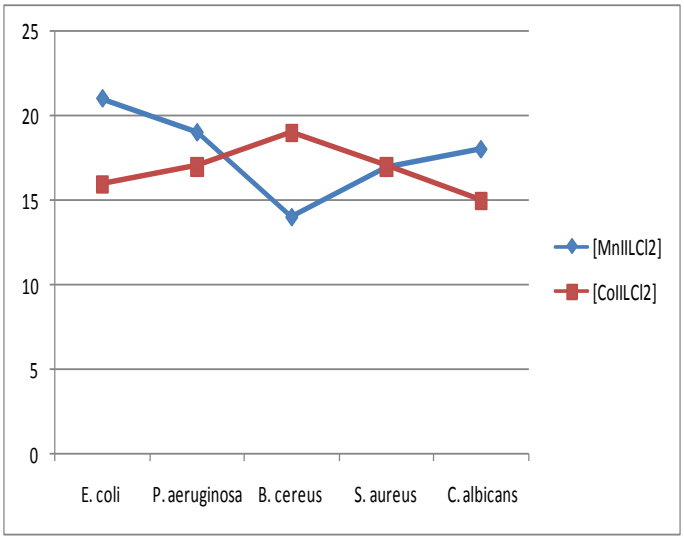

Fig. 6. Graphical presentation of antimicrobial activity of the macrocyclic complexes against pathogens

Table 4. Antimicrobial activity of $[Mn^{II}LCl_2]$ and $[Co^{II}LCl_2]$ macrocyclic complexes

Complex (100 mg/ml)	**Diameter of inhibition zone (mm)**				
	E. coli	***P. aeruginosa***	***B. cereus***	***S. aureus***	***C. albicans***
$[Mn^{II}LCl_2]$	21	19	14	17	18
$[Co^{II}LCl_2]$	16	17	19	17	15
Gentamycin	24	24	24	24	20

Antimicrobial activity for both macrocyclic complexes were evaluated by measuring the zone of growth inhibition against the pathogens with zone reader (Hi Antibiotic Zone Scale) [27-29]. The $[Mn^{II}LCl_2]$ macrocyclic complex showed maximum zone of inhibition against *E. coli* (21 mm) followed by *P. aeruginosa* (19 mm), *B. cereus* (14 mm) and *S. aureus* (17 mm). $[Co^{II}LCl_2]$ macrocyclic complex exhibit maximum zone of inhibition against *B. cereus* (19 mm) followed by *E. coli* (14 mm), *P. aeruginosa* (17 mm) and *S. aureus* (17 mm). Against fungal pathogen *C. albicans*, $[Mn^{II}LCl_2]$ macrocyclic complex was found most effective (18 mm) followed by the $[Co^{II}LCl_2]$ macrocyclic complex (15 mm) as showed in Fig. 6 and the observed data given in Table 4.

4. CONCLUSION

In present work, pentaazamacrocyclic complexes of Mn(II) and Co(II) have been synthesized by the template method using 1 mole of TETA (0.292 gm/0.31 ml), 1 mole of 2,6-diacetyl pyridine (0.326 g) and 1 mole of metal salts [$MnCl_2.4H_2O$ (0.198 gm)/ $CoCl_2.6H_2O$ (0.476 gm)]. Spectral studies have confirmed the saddle-shape octahedral geometry for these macrocyclic complexes. Cyclic voltammetric studies showed the interesting results for their unusual oxidation states. The studies of voltammetric chemical quantum parameters of these macrocyclic complexes by using $E_{HOMO/LUMO}$ energies showed that these macrocyclic complexes are globally hard and stable. Antimicrobial activity of $[Mn^{II}LCl_2]$ and $[Co^{II}LCl_2]$ macrocyclic complexes showed that $[Mn^{II}LCl_2]$ macrocyclic complex is most potent against *E. coli* with respect to standard drug Gentamycin.

Acknowledgements

The authors are thankful to CSIR New Delhi for financial support in the past projects and support is also acknowledged for completing of these studies from SAIF Panjab University Chandigarh and IIT Roorkee.

REFERENCES

[1] S. Chandra, S. Verma, U. Dev, and N. Joshi, J. Coord. Chem. 62 (2009) 1327.
[2] A. Chaudhary, N. Bansal, A. Gajraj, and R.V. Singh, J. Inorg. Biochem. 96 (2003) 393.
[3] G. A. Melson (Ed.) Coordination Chemistry of Macrocyclic Compounds, Plenum Press, New York (1979).
[4] A.Kumar, and R. Singh, Anal. Bioanal. Electrochem. 8 (2016) 382.
[5] A. Kumar, P. Tevatia, Sweety, and R. Singh, Der Pharm. Chem. 8 (2016) 146.
[6] R. H. Dixon (Ed.) Reproductive Toxicology, Raven Press, New York (1985) p. 309.

[7] A. H. EL. Boraey, M. E. Sanaa, A. T. Dina, and M. A. L. Nahas, Spectrachim. Acta Part A 78 (2011) 360.
[8] A. H. EL. Boraey and O. A. EL. Gammal, Spectrachimica Acta Part A 138 (2015) 553.
[9] M. A. Baseer, V. D. Jadhav, R. M. Phule, Y. V. Archana, and Y. B. Vibhute, Orient. J. Chem 16 (2000) 553.
[10] P. A. Ajibade, and N. H. Zulu, Int. J. Mol. Sci. 12 (2011) 7186.
[11] P. M. Reddy, R. R., E. R. Krishna, A. Hu, and V. Ravinder, Int. J. Mol. Sci. 13 (2012) 4982.
[12] E. Unur, L. Toppare, Y. Yagci, and F. Yalmaz, J. Appl. Poly. Sci. 95 (2005) 1014.
[13] C. J. Brabec, S. Gowrisanker, J. J. M. Halls, D. Laird, S. Jia, and S. P. Williams, Adv. Mater. 22 (2010) 3839.
[14] P. Tevatia, A. Kumar, Sweety, and R. Singh, J. Bas. Appl. Eng. Res. 2 (2015) 924.
[15] A. Kumar, Sweety, P. Tevatia, M. Agarwal, and Singh, R., Int. J. Pharm. Chem. 5 (2015) 4.
[16] S. Reineke, F. Lindner, G. Schwartz, N. Seidler, K. Walzer, B. Lüssem, and K. Leo, Nature 459 (2009) 234.
[17] H. Sasabe, J. I. Takamatsu, T. Motoyama, S. Watanabe, G. Wagenblast, N. Langer, O. Molt, E. Fuchs, C. Lennartz, and J. Kido, Adv. Mater. 22 (2010) 5003.
[18] R. Holmes, B. D. Andrade, S. Forrest, X. Ren, J. Li, and M. Thompson, Appl. Phys. Lett. 83 (2003) 3818.
[19] E. V. Tsiper, Z. G. Soos, W. Gao, and A. Kahn, Chem. Phys. Lett. 360 (2002) 47.
[20] K. Reem Shah, S. Khlood Abou-Melha, A. Fawaz Saad, T. Yousef, A. A. Gamil Al-Hazmi, G. Marwa Elghalban, M. Abdalla Khedr, and N. El-Metwaly, J. Therm. Anal. Calorim. 15 (2015) 4838.
[21] U. El. Ayaan, M. M. Youssef, and A. S. Shihry, J. Mol. Struct. 936 (2009) 213.
[22] R. G. Pearson, J. Org. Chem. 54 (1989) 1423.
[23] J. Padmanabhan, R. Parthasarathi, and V. Subramanian, J. Phys. Chem. A 111 (2007) 1358.
[24] R. H. Friend, R. W. Gymer, A. B. Holmes, and J. H. Burroughes, Nature 347 (1990) 121.
[25] T. Mori, H. Takeuchi, and H. Fujikawa, J. Appl. Phys. 97 (2005) 66102.
[26] T. Oyamada, H. Tanaka, K. Matsushige, H. Sasabie, and C. Adachi, Appl. Phys. Lett. 83 (2003) 1252.
[27] S. Riechel, C. Kallinger, U. Lemmer, J. Feldmann, A. Gombert, V. Wittwer, and U. Scherf, Appl Phy. Lett. 77 (2000) 2310.
[28] D. Andrade, S. Datta, S. Forrest, P. Djurovich, E. Polikarpov, and M. Thompson, Org. Electron. 6 (2005) 11.
[29] M. Xu, R. Zhou, G. Wang, and J. Yu, Inorg. Chim. Acta 362 (2009) 515.

[30] B. W. D. Andrade, S. Datta, S. R. Forrest, and P. Djurovich, E. Polikarpov, M. E. Thompson, Org. Electron. 6 (2005) 11.
[31] G. Cynthia Zoski, Handbook of Electrochemistry, Elsevier, Oxford (2007) p. 892.
[32] J. H. Burroughes, D. D. C. Bradley, A. R. Brown, R. N. Marks, K. Mackay, R. H. Friend, P. L. Burn, and A. B. Holmes, Nature 347 (1990) 539.
[33] M. Beija, C. A. M. Afonso, and J. M. G. Martinho, Chem. Soc. Rev. 38 (2009) 2410.
[34] G. B. Ferreira, E. Hollauer, N. M. Comerlato, and J. Wardell, Spectrochim. Acta Part A 71 (2008) 215.
[35] L. K. Gupta, U. Bansal, and S. Chandra, Spectrochim. Acta A 65 (2006) 463.
[36] P. Tevatia, A. Kumar, Sweety, and R. Singh, J. Appl. Chem. 7 (2014) 51.
[37] Sweety, A. Kumar, P. Tevatia, and R. Singh, J. Chem. Pharm. Res. 8 (2016) 444.